EAGE

CONFERENCE & EXHIBITION
NEAR SURFACE GEOSCIENCE'21

Distributed acoustic sensing of daylight on a glacier in Canada: hotspot monitoring

R. Ferguson[1], C. Mosher[2], J. Dettmer[1], J. Mish[1]

[1] Department of Geoscience, University of Calgary; [2] MoMacMo

Summary

Decomposition of 30 days of continuous DAS acquisition reveals a temperature signature that correlates with sunrise and sunset in the sub-1 Hz frequency band. The acquisition surface consists of glacier, glacial margin and exposed rock and soil. Characteristic DAS intensities of the DAS response to sunrise correlate with on-glacier and off-glacier respectively. We speculate that glacial advance and retreat in realtime is detectable using DAS.

Introduction

A recent acquisition program conducted at the Mount Meager glacier in Canada utilizes a Distributed Acoustic Sensing (DAS) system to monitor this increasingly active volcanic region. Thirty days of data are acquired to capture seismic characteristics associated with rock falls and other strain events. Though the capture of high-frequency seismic signatures in the DAS data recorded at Meager were previously considered (Klaasen et al., submitted 2021), we consider long-period signals here with the goal to study temperature effects at frequencies below about 1 Hz. This temperature response is interesting because conventional DAS acquisition based on Rayleigh scattering of laser light within a fibre optic cable associates the captured laser intensities with strain on the cable (Nakazawa et al., 1981; Rogers and Handerek, 1992, for example). Some recent examples of strain / DAS measurements include Krawczyk et al. (2020), who use existing fibre-optic infrastructure at the Etna volcano to monitor seismic and volcanic activity in the surrounding area; Nishimura et al. (2021) capture DAS signals associated with volcanic bombs and ash in realtime, and DAS finds use in geothermal modelling because it is a fast / cheap alternative to 4D-seismic imaging (Mondanos and Coleman, 2019; Raab et al., 2019; Lellouch et al., 2020). Conventional temperature sensors based on fibre optics exist, but they are based on Raman scattering (Measures and Abrate, 2002, for example), and so separate temperature and strain systems are usually deployed to capture both measurements. In this abstract, we use wavelet decomposition of the DAS data using Mosher (2012) to isolate the sub-1Hz frequency content and its variation in time. Using the astronomical algorithms summarized in Meeus (1998), we compute sunrise and sunset times for each of the 380 DAS 'stations' for all 30 days. We find a good correlation between sunrise and a sudden intensity variation in the DAS data.

Method

To verify the correlation between daylight with intensity variation in the DAS cable, we calculate the variation of solar elevation in time relative to the position and local topography for each of the 380 DAS stations. The acquisition layout at Mount Meager is given in Figure 1 as a series of red dots, and the contours indicate the angle of elevation in degrees between a station (stn 170 / 380) and points in the surrounding topography. The dashed black-lines indicate the azimuths of sunrise and sunset from the perspective of stn 170, with $\triangle$ and $\triangledown$ indicating the points where the sun rises over the elevation (the topographic sunrise and sunset respectively). Figures 1(a) and Figures 1(b) correspond to the first day of acquisition (September 18, 2019) and the final day (October 17, 2019) respectively; the solar azimuths change significantly over the 30 days of acquisition and so the topographic sunrise and sunsets change accordingly. The solar azimuths and elevations are calculated according to Meeus (1998) and then corrected based on the elevation of each station and the elevations of the surrounding topography. Figure 2 gives examples of solar elevation and topographic elevation from the perspective of station 170 along the solar azimuth as it varies through the day. Figure 2(a) indicates that the Sept. 18 sunrise (the solar elevation > 0 degrees) occurs at minute 414 and that the elevation of the local topography is below 0 degrees so that stn 170 is illuminated at minute 414 ($\triangle$ on Figure 1(a)). The solar elevation rises through the morning until about minute 463 where the local topography casts a brief shadow. Sunset occurs at minute 1150 but the topographic sunset occurs earlier at about 1093 where the sun dips below the local topography ($\triangledown$ on Figure 1(a)). Sunrise and sunset occur at approximately 430 minutes and 1100 minutes respectively on the final acquisition day (Oct. 17), but the topographic sunrise and sunset occur earlier at 520 minutes and 1020 minutes respectively. Our purpose, then, is to compare our topographic sunrises and sunsets for each station for each day to the DAS data.

Examples

We decompose the DAS data into its constituent frequency bands following Mosher (2012) and here we concentrate on the < 1 Hz band. Figure 3 give the DAS data associated with September 30, 2019 plus the corresponding temperature for that day from a nearby weather station. Topographic sunrise (solid line) and sunset (dashed line) for that day are plotted in Figure 3(a) and we see that there is a good correlation between sunrise and a strong intensity increase in the DAS data for the region circled in green. The correlation breaks down somewhat due to what appears to be topographic shadowing as is indicated by

the red circle; the topographic map that we base our elevations on is quite sparse, and we expect that the correlation will improve with the adaption of a topographic map from a lidar reconnaissance. Sunset seems to provoke a weak or perhaps negligible intensity response in the DAS data in Figure 3(a); the temperature data in Figure 3(b) (from a nearby weather station) indicate that sunrise causes a sudden rise in the atmospheric temperature that sunset does not.

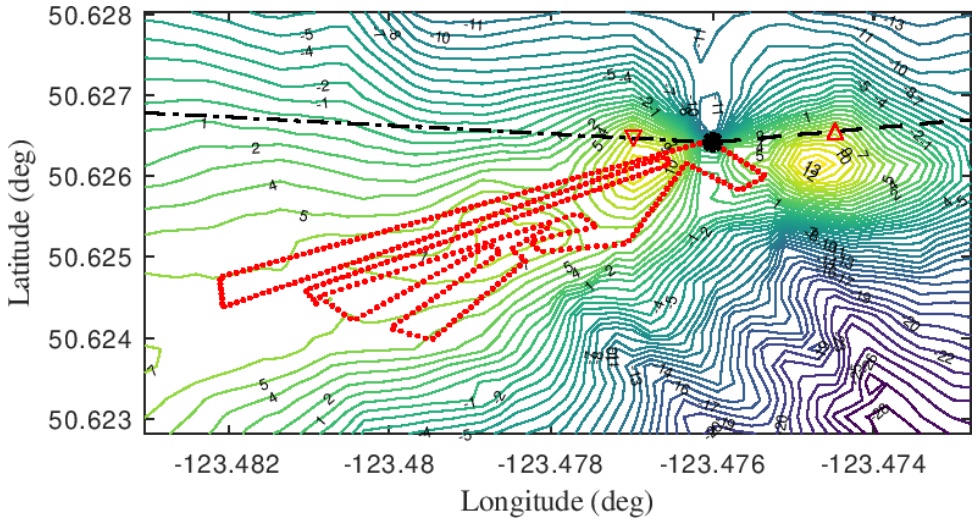

(a)

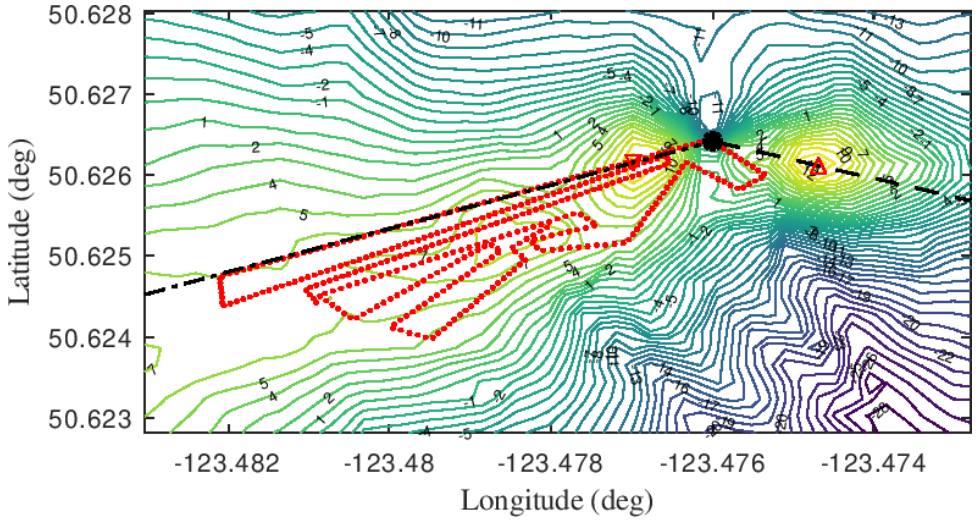

(b)

Figure 1 *Contour map of elevation angles for station 170 (the "•" symbol) on Sept. 18, 2019 (a) and Oct. 17, 2019 (b). The sun rises along the dashed line in the East above the elevation high-point indicated by* △ *, and then it sets at* ▽ *along the "· - ·" azimuth.*

Conclusions

We find a correlation between a strong intensity increase in DAS data that corresponds to sunrise. The DAS data were acquired on a glacier atop Mount Meager in Canada and and processed using wavelet decomposition into a sub 1 Hz data volume. Astronomical algorithms provided solar location and time relative to each station in the survey for all thirty days of acquisition, and we corrected the corresponding sunrise and sunset times for the local topography. The good correlation that we find on one set of DAS stations is partially offset by a more vague correlation for a smaller set of stations that we hope to resolve through the adaption of a high density lidar survey. With the relationship between sunrise temperature and DAS intensity established, we will attempt to quantify a temperature / intensity relationship that

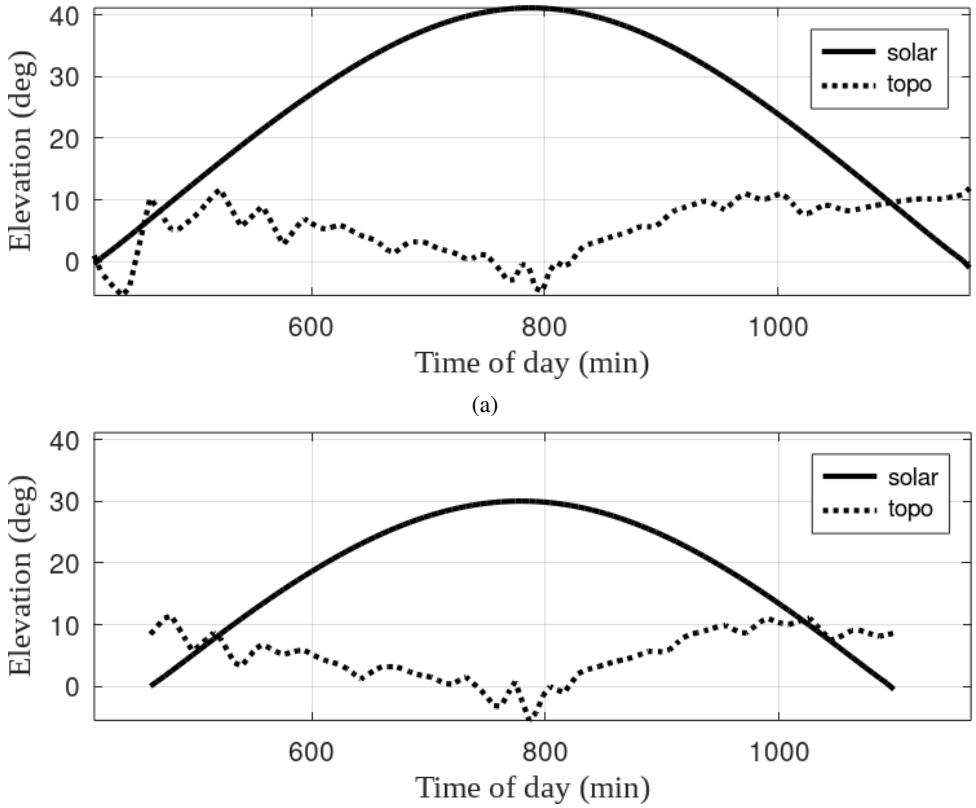

Figure 2 *Solar elevation (solid line) and topographic elevation (dotted line) in degrees vs. time of day for station 170. a) Sunrise on Sept. 18, 2019 occurs at minute 414 when the solar elevation is greater than zero (is above the horizon) with a shadow around minute 463 due to topography nearby (symbol "△" on Figure 1(a)). Continuous daylight ends at minute 1096 when the sun sets below the topography (symbol "▽" on Figure 1(b)). b) The sun rises above the topography at minute 520 on Oct. 17, 2019 and sets at minute 1020.*

might be useful in the separation of diurnal variations in DAS intensity from geologic and geothermally induced variations.

Acknowledgements

This work was supported by MoMacMo (an AWS based not-for profit geophysical processing organizartion) and the Government of Canada's New Frontiers in Research Fund (NFRF), Geoscience BC, the Natural Resources Canada Emerging Renewable Power Program, and the Geological Survey of Canada Geoscience for New Energy Program.

References

Klaasen, S., Paitz, P., Lindner, N., Dettmer, J. and Fichtner, A. [submitted 2021] Distributed Acoustic Sensing in Volcano-Glacial Environments - Mount Meager, British Columbia. *Journal of geophysical research: Solid earth.*

Krawczyk, C., Jousset, P., Currenti, G., Weber, M., Napoli, R., Reinsch, T., Riccobene, G., Zuccarello, L., Chalari, A. and Clarke, A. [2020] Monitoring volcanic and seismic activity with multiple fibre-optic Distributed Acoustic Sensing units at Etna volcano. In: *EGU General Assembly 2020*. European Geophysical Union, 1.

Lellouch, A., Lindsey, N.J., Ellsworth, W.L. and Biondi, B.L. [2020] Comparison between distributed acoustic sensing and geophones; downhole microseismic monitoring of the FORGE geothermal experiment. *Seismological research letters*, **91**(6), 3256–3268.

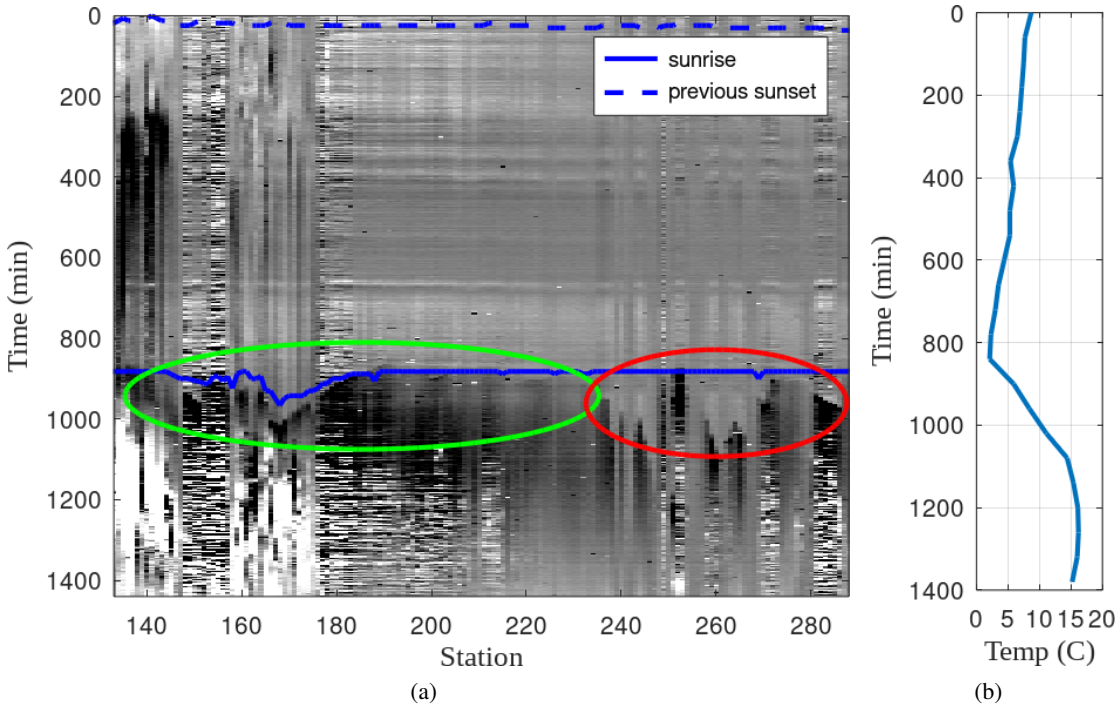

Figure 3 *DAS, daylight and temperature. a) DAS data from September 30, 2019 plotted with sunrise (solid line) and sunset from September 29, 2019 (dashed line). The green and red ellipses correspond, respectively, to regions where the sunrise correlates and does not correlate with changes in DAS intensity. b) Hourly temperature from the closest weather station. Though the station lies approximately 1000m below in a valley, a sudden temperature increase at about 820 minutes corresponds well with the sunrise signal.*

Measures, R. and Abrate, S. [2002] Structural Monitoring with Fiber Optic Technology. *Applied mechanics reviews*, **55**(1), B10–B11.

Meeus, J. [1998] *Astronomical algorithms*. Willmann-Bell, Richmond, Va.

Mondanos, M. and Coleman, T. [2019] Application of distributed fibre-optic sensing to geothermal reservoir characterization and monitoring. *First Break*, **37**(7), 51–56.

Mosher, C.C. [2012] Generalized Windowed Transforms for Seismic Processing And Imaging. In: *SEG Technical Program Expanded Abstracts 2012*. Society of Exploration Geophysicists, 1–4.

Nakazawa, M., Horiguchi, T., Tokuda, M. and Uchida, N. [1981] Measurement and analysis on polarization properties of backward Rayleigh scattering for single-mode optical fibers. *IEEE Journal of Quantum Electronics*, **17**(12), 2326–2334.

Nishimura, T., Emoto, K., Nakahara, H., Miura, S., Yamamoto, M., Sugimura, S., Ishikawa, A. and Kimura, T. [2021] Source location of volcanic earthquakes and subsurface characterization using fiber-optic cable and distributed acoustic sensing system. *Scientific reports*, **11**(1), 6319–6319.

Raab, T., Reinsch, T., Aldaz Cifuentes, S.R. and Henninges, J. [2019] Real-Time Well-Integrity Monitoring Using Fiber-Optic Distributed Acoustic Sensing. *SPE journal (Society of Petroleum Engineers (U.S.) : 1996)*, **24**(5), 1997–2009.

Rogers, A.J. and Handerek, V.A. [1992] Frequency-derived distributed optical-fiber sensing: Rayleigh backscatter analysis. *Applied Optics*, **31**(21), 4091–4095.